Article

Oligo(*N*-aryl glycines): A New Twist on Structured Peptoids

Neel H. Shah, Glenn L. Butterfoss, Khanh Nguyen, Barney Yoo,
Richard Bonneau, Dallas L. Rabenstein, and Kent Kirshenbaum

J. Am. Chem. Soc., **2008**, 130 (49), 16622-16632 • DOI: 10.1021/ja804580n • Publication Date (Web): 17 November 2008

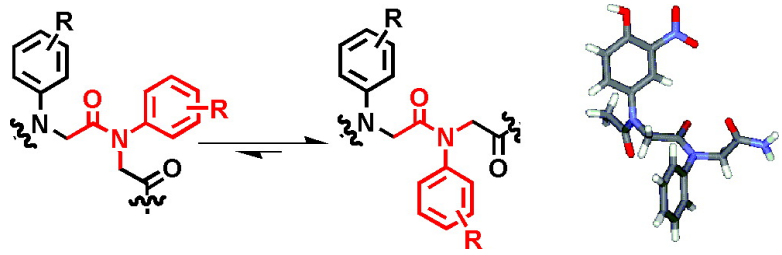

J|A|C|S
ARTICLES

Published on Web 11/17/2008

Oligo(*N*-aryl glycines): A New Twist on Structured Peptoids

Neel H. Shah,[†] Glenn L. Butterfoss,[‡,§] Khanh Nguyen,[||] Barney Yoo,[†] Richard Bonneau,[‡,§] Dallas L. Rabenstein,[||] and Kent Kirshenbaum*[,†]

Department of Chemistry, Center for Genomics & Systems Biology, and Courant Institute of Mathematical Sciences, Department of Computer Science, New York University, New York, New York 10003, and Department of Chemistry, University of California, Riverside, California 92521

Received June 16, 2008; E-mail: kent@nyu.edu

Abstract: We explore strategies to enhance conformational ordering of N-substituted glycine peptoid oligomers. Peptoids bearing bulky *N*-alkyl side chains have previously been studied as important examples of biomimetic "foldamer" compounds, as they exhibit a capacity to populate helical structures featuring repeating cis-amide bonds. Substantial cis/trans amide bond isomerization, however, gives rise to conformational heterogeneity. Here, we report the use of *N*-aryl side chains as a tool to enforce the presence of trans-amide bonds, thereby engendering structural stability. Aniline derivatives and bromoacetic acid are used in the facile solid-phase synthesis of a diverse family of sequence-specific *N*-aryl glycine oligomers. Quantum mechanics calculations yield a detailed energy profile of the folding landscape and substantiate the hypothesis that the presence of anilide groups establishes a strong energetic preference for trans-amide bonds. X-ray crystallographic analysis and solution NMR studies verify this preference. Molecular modeling indicates that the linear oligomers can adopt helical structures resembling a polyproline type II helix. High resolution structures of macrocyclic oligomers incorporating both *N*-alkyl and *N*-aryl glycine units confirm the ability to direct the presence of trans-amide bonds specifically at *N*-aryl positions. These results are an important step in developing strategies for the rational de novo design of new structural motifs in biomimetic oligopeptoid systems.

Introduction

The de novo design of heteropolymer chains with predictable folded structures is a formidable challenge for researchers in the fields of both biopolymer and synthetic polymer chemistry. Within the context of protein design, each individual amino acid residue can assume several distinct backbone and side chain dihedral angles. It is difficult, therefore, to determine a priori particular amino acid sequences that will favor one set of these angles over the multitude of alternatives. For proteins, however, the numerous structures deposited in the Protein Data Bank facilitate the rational design of sequences that are compatible with a desired backbone topology.[1] In contrast, detailed structural information for non-natural sequence-specific oligomers is limited, but growing. The study of folding principles in these synthetic systems is now under active investigation.[2] A variety of synthetic oligomers have been described that exhibit a propensity to form stable secondary structures.[3−5] These "foldamers" show promise for applications in biomedicine and materials science.[6,7] Investigating the conformational preferences of foldamers and their constituent monomer sets is a critical

[†] Department of Chemistry, New York University.
[‡] Center for Genomics & Systems Biology, New York University.
[§] Department of Computer Science, New York University.
[||] University of California.

(1) (a) Byrson, J. W.; Betz, S. F.; Lu, H. S.; Suich, D. J.; Zhou, H. X.; O'Neil, K. T.; DeGrado, W. F. *Science* **1995**, *270*, 935–941. (b) Ho, S. P.; DeGrado, W. F. *J. Am. Chem. Soc.* **1987**, *109*, 6751–6758. (c) Regan, L.; DeGrado, W. F. *Science* **1988**, *241*, 976–978. (d) Ramirez-Alvarado, M.; Blanco, F. J.; Serrano, L. *Nat. Struct. Biol.* **1996**, *3*, 604–612. (e) Dahiyat, B. I.; Mayo, S. L. *Science* **1997**, *278*, 82–87. (f) Schafmeister, C. E.; LaPorte, S. L.; Miercke, L. J. W.; Stroud, R. M. *Nat. Struct. Biol.* **1997**, *4*, 1039–1046. (g) Dalal, S.; Balasubramanian, S.; Regan, L. *Nat. Struct. Biol.* **1997**, *4*, 548–552. (h) Chin, J. W.; Schepartz, A. *J. Am. Chem. Soc.* **2001**, *123*, 2929–2930. (i) Ottesen, J. J.; Imperiali, B. *Nat. Struct. Biol.* **2001**, *8*, 535–539. (j) Kuhlman, B.; Dantas, G.; Ireton, G.; Varani, G.; Stoddard, B. L.; Baker, D. *Science.* **2003**, *302*, 1364–1368. (k) Huang, P.-S.; Love, J. J.; Mayo, S. L. *Protein Sci.* **2007**, *16*, 2770–2774.

(2) (a) Dill, K. A.; Bromberg, S.; Yue, K.; Fiebig, K. M.; Yee, D. P.; Thomas, P. D.; Chan, H. S. *Protein Sci.* **1995**, *4*, 561–602. (b) Gellman, S. H. *Acc. Chem. Res.* **1998**, *31*, 173–180. (c) Hill, D. J.; Mio, M. J.; Prince, R. B.; Hughes, T. S.; Moore, J. S. *Chem. Rev.* **2001**, *101*, 3893–4011. (d) Goodman, C. M.; Choi, S.; Shandler, S.; DeGrado, W. F. *Nat. Chem. Biol.* **2007**, *3*, 252–262. (e) *Foldamers: Structure, Properties, and Applications*; Hecht, S.; Huc, I. Eds.; Wiley-VCH: Weinheim, Germany, 2007.

(3) (a) Seebach, D.; Overand, M.; Kuhnle, F. N. M.; Martinoni, B.; Oberer, L.; Hommel, U.; Widmer, H. *Helv. Chim. Acta* **1996**, *4*, 913–941. (b) Appella, D. H.; Christianson, L. A.; Karle, I. L.; Powell, D. R.; Gellman, S. H. *J. Am. Chem. Soc.* **1996**, *118*, 13071–13072. (c) Appella, D. H.; Christianson, L. A.; Klein, D. A.; Powell, D. R.; Huang, X, Jr.; Gellman, S. H. *Nature* **1997**, *387*, 381–384. (d) Hintermann, T.; Seebach, D. *Synlett* **1997**, 437–438. (e) Cheng, R. P.; Gellman, S. H.; DeGrado, W. F. *Chem. Rev.* **2001**, *101*, 3219–3232. (f) Daniels, D. S.; Petersson, J.; Qiu, J. X.; Schepartz, A. *J. Am. Chem. Soc.* **2007**, *129*, 1532–1533.

(4) (a) Nelson, J. C.; Saven, J. G.; Moore, J. S.; Wolynes, P. G. *Science* **1997**, *30*, 402–413. (b) Oh, K.; Jeong, K.-S.; Moore, J. S. *Nature* **2001**, *414*, 889–893. (c) Arnt, L.; Tew, G. N. *J. Am. Chem. Soc.* **2002**, *124*, 7664–7665. (d) Okhita, M.; Lehn, J.-M.; Baum, G.; Fenske, D. *Chem.—Eur. J.* **1999**, *5*, 3471–3481. (e) Estroff, L. A.; Incarvito, C. D.; Hamilton, A. D. *J. Am. Chem. Soc.* **2004**, *126*, 2–3. (f) Dolain, C.; Leger, J.-M.; Delsuc, N.; Gornitzka, H.; Huc, I. *Proc. Natl. Acad. Sci.* **2005**, *102*, 16146–16151.

10.1021/ja804580n CCC: $40.75

initial step in understanding the sequence–structure relationships that can guide the predictable design of diverse folded architectures.

The construction of sequence-specific oligomers with well-defined conformations typically relies on one of two design concepts. The first strategy is to employ flexible oligomer systems that can establish long-range noncovalent interactions to direct folding. This is evident in biopolymers, where hydrogen bonding and hydrophobic interactions aid in defining protein structures.[8] These interactions are also seen in non-natural oligomers, in particular β-peptides, whose diverse secondary structures can be defined by various intramolecular hydrogen-bonding patterns.[3] The second design strategy is to use oligomers incorporating rigid monomer units with conformationally constrained linkages. This method allows for predictable organization of the oligomer backbone through local conformational preferences. For example, the semirigid covalent linkages between monomer units in oligo(*m*-phenylene-ethynylenes) predispose the oligomers to form helical conformations.[4a−c]

We adopt a general approach for designing complex self-assembled structures in biomimetic macromolecules that entails, first, the discovery of monomer types predisposed to generate well-defined conformations that can be propagated through local interactions upon oligomerization; second, an effort to solve three-dimensional structures of diverse oligomer sequences in order to describe these conformations; third, the use of computational tools employing an energy function to sample conformational space and evaluate variations in conformational preferences for different oligomer sequences. Implementation of this strategy would then rely upon an iterative process to guide the synthesis of increasingly complex structures. In practice, analysis of experimental findings can ensure the suitability of the computational tools, and the energy function in turn can guide subsequent generations of oligomer sequences. This study embarks upon such an approach.

Our investigations are focused on a class of peptidomimetics known as peptoids. These oligomers are composed of a wide variety of N-substituted glycine monomer units that can be efficiently linked in a sequence-specific manner.[9] Cursory inspection would suggest that peptoids are poor candidates for folding. The peptoid backbone repeating unit includes a methylene group which can confer flexibility, and there is no intrinsic capacity within the backbone to establish long-range interactions, as there are no hydrogen-bond donors (Scheme 1). Nevertheless, the incorporation of bulky, branched *N*-alkyl substituents has been shown to generate local steric interactions that can direct conformational preferences.[10a] A variety of peptoids bearing these side chains exhibit a polyproline type I helical secondary structure with repeating cis-amide bonds.[5,10] In solution, however, this structure is the dominant member of a multiconformational ensemble.[5,10c]

Scheme 1. Comparison of Peptide and Peptoid Structures

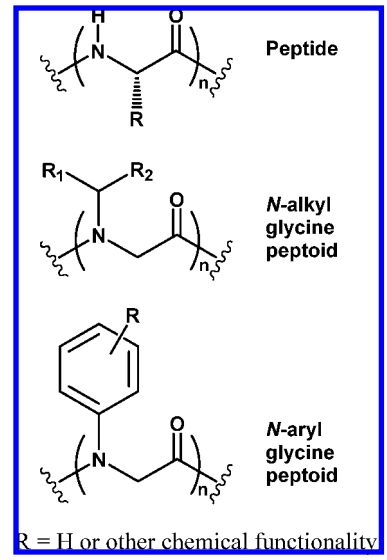

A critical impediment to the design of peptoids with stable secondary structures is that there is substantial conformational heterogeneity associated with the ability to populate both cis- and trans-amide bond geometries.[10c] Peptoids bearing bulky, branched *N*-alkyl side chains exhibit only a modest energetic preference for cis-amide bonds, with a cis−trans-free energy difference typically under 1 kcal/mol.[10a,11] Efforts have been made to modulate this conformational preference by tuning stereoelectronic interactions between proximal backbone amide groups and side chains.[11b] In short oligomers, however, this approach generally does not yield energetic preferences substantially above 1 kcal/mol. It is not yet evident if such energy differences between cis- and trans-amide bonds will be sufficient to establish conformational homogeneity in longer oligomers. Alternatively, strategies have been explored to establish long-range constraints that can better define peptoid backbone conformation. One strategy that has proven effective in reducing

(5) Armand, P.; Kirshenbaum, K.; Goldsmith, R. A.; Farr-Jones, S.; Barron, A. E.; Truong, K. T. V.; Dill, K. A.; Mierke, D. F.; Cohen, F. E.; Zuckermann, R. N.; Bradley, E. K. *Proc. Natl. Acad. Sci. U.S.A.* **1998**, *95*, 4309–4314.
(6) (a) Murphy, J. E.; Uno, T.; Hamer, J. D.; Cohen, F. E.; Dwarki, V.; Zuckermann, R. N. *Proc. Natl. Acad. Sci.* **1998**, *95*, 1517–1522. (b) Werder, M.; Hauser, H.; Abele, S.; Seebach, D. *Helv. Chim. Acta* **1999**, *82*, 1774–1783. (c) Kritzer, J. A.; Lear, J. D.; Hodsdon, M. E.; Schepartz, A. *J. Am. Chem. Soc.* **2004**, *126*, 9468–9469. (d) Arnt, L.; Nusslein, K.; Tew, G. N. *J. Polym. Chem., Part A* **2004**, *42*, 3860–3864. (e) Yin, H.; Frederick, K. K.; Liu, D.; Wand, J.; DeGrado, W. F. *Org. Lett.* **2006**, *8*, 223–225.
(7) (a) Bekele, H.; Fendler, J. H.; Kelly, J. W. *J. Am. Chem. Soc.* **1999**, *121*, 7266–7267. (b) Cuccia, L. A.; Ruiz, E.; Lehn, J. M.; Homo, J. C.; Schmutz, M. *Chem.—Eur. J.* **2002**, *8*, 3448–3457. (c) Hou, J.-L; Yi, H.-P.; Shao, X.-B.; Li, C.; Wu, Z.-Q.; Jiang, X.-K.; Wu, L.-Z.; Tung, C.-H.; Li, Z.-T. *Angew. Chem., Int. Ed.* **2006**, *45*, 796–800. (d) Brown, N. J.; Wu, C. W.; Seurynck-Servoss, S. L.; Barron, A. E. *Biochemistry* **2008**, *47*, 1808–1818.
(8) (a) Pauling, L.; Corey, R. B.; Branson, H. R. *Proc. Natl. Acad. Sci. U.S.A.* **1951**, *37*, 205–211. (b) Dill, K. A. *Biochemistry* **1990**, *29*, 7133–7155. (c) Chan, H. S.; Dill, K. A. *Annu. Rev. Biophys. Biophys. Chem.* **1991**, *20*, 447–490.
(9) Zuckermann, R. N.; Kerr, J. M.; Kent, S. B. H.; Moos, W. H. *J. Am. Chem. Soc.* **1992**, *114*, 10545–10647.
(10) (a) Armand, P.; Kirshenbaum, K.; Falicov, A.; Dunbrack, R. L.; Dill, K. A.; Zuckermann, R. N.; Cohen, F. E. *Folding Des.* **1997**, *2*, 369–375. (b) Kirshenbaum, K.; Barron, A. E.; Goldsmith, R. A.; Armand, P.; Bradley, E. K.; Truong, K. T. V.; Dill, K. A.; Cohen, F. E.; Zuckermann, R. N. *Proc. Natl. Acad. Sci. U.S.A.* **1998**, *95*, 4303–4308. (c) Wu, C. W.; Kirshenbaum, K.; Sanborn, T. J.; Patch, J. A.; Huang, K.; Dill, K. A.; Zuckermann, R. N.; Barron, A. E. *J. Am. Chem. Soc.* **2003**, *125*, 13525–13530.
(11) (a) Sui, Q.; Borchardt, D.; Rabenstein, D. L. *J. Am. Chem. Soc.* **2007**, *129*, 12042–12048. (b) Gorske, B. C.; Bastian, B. L.; Geske, G. D.; Blackwell, H. E. *J. Am. Chem. Soc.* **2007**, *129*, 8928–8929.
(12) (a) Shin, S.-B.Y.; Yoo, B.; Todaro, L.; Kirshenbaum, K. *J. Am. Chem. Soc.* **2007**, *129*, 3218–3225. (b) Holub, J. M.; Jang, H.; Kirshenbaum, K. *Org. Lett.* **2007**, *9*, 3275–3278. (c) Maulucci, N.; Izzo, I.; Bifulco, G.; Aliberti, A.; De Cola, C.; Comegna, D.; Gaeta, C.; Napolitano, A.; Pizza, C.; Tedesco, C.; Flot, D.; De Riccardis, F. *Chem. Commun.* **2008**, 3927–3929.

Scheme 2. Amide Bond Geometry in Peptides and Peptoids[a]

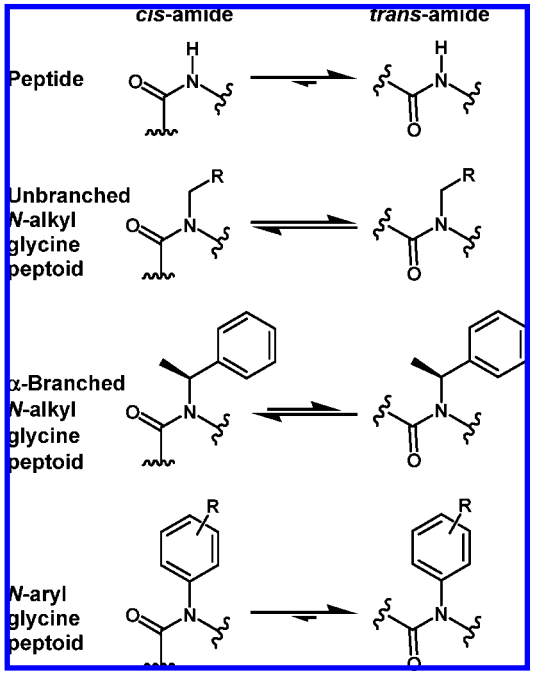

[a] The cis/trans notation for peptoid amide groups is chosen for consistency with the notation for polypeptides and proteins, although E/Z notation could also be applied.

peptoid conformational heterogeneity is the inclusion of covalent macrocyclic constraints.[12] Head-to-tail cyclized peptoid oligomers can be synthesized with high efficiency and result in products that exhibit sufficient conformational ordering to yield X-ray crystal structures.[12a,c] Although this strategy has proven effective in defining a new series of stable peptoid conformations, it is limited to cyclic products.

We are developing new tools to control peptoid conformations, thereby expanding the scope of accessible secondary, tertiary, and quaternary structures. We seek readily available, chemically diverse monomer types that establish intramolecular interactions and lead to predictable sequence-structure relationships. Previous structural investigations of peptoids have focused on the use of relatively flexible *N*-alkyl glycine monomer units that may confound the design of well-defined peptoid folds. This study evaluates the conformational properties of *N*-aryl glycine peptoids (Scheme 1). Bradley and co-workers initially suggested that the incorporation of *N*-aryl peptoid side chains may reduce conformational heterogeneity; however, this phenomenon was not analyzed further.[13] Here, we present an experimental and computational evaluation of *N*-aryl side chains, establishing that the inclusion of these groups within peptoid oligomers provides a strong energetic preference for trans-amide bond geometries (Scheme 2). We demonstrate that *N*-aryl glycine building blocks can be used to generate new peptoid secondary structures that are conformationally defined in solution. This new family of peptoid structures may facilitate the de novo design of chemically diverse biomimetic architectures.

Results and Discussion

The Conformation of *N*-Methylacetanilides. We conducted a computational study of *N*-methylacetanilide, the smallest structural unit representative of the amide bond found in *N*-aryl peptoids. Pedersen et al. showed in the 1960s that the stable conformation of this small organic molecule, both in solution and in its crystalline state, displayed the amide oxygen trans to the phenyl ring ($\omega \approx 180°$), with the phenyl ring perpendicular to the plane of the amide bond ($\chi_1 \approx 90°$) (Scheme 3).[14] We sought to determine the energetic difference between the cis- and trans-amide isomers and thus verify the utility of ab initio quantum mechanics calculations in evaluating the conformational preferences of small peptoid-resembling structures. *N*-methylacetanilide was allowed to freely minimize at the HF/G-31G* level of theory from both cis- and trans-amide starting structures. The geometry of the optimized trans-amide structure displayed the same dihedral angles as previously determined by experiment (Figure 1). Energy calculations using HF, B3LYP, and MP2 methods consistently establish that a trans-amide bond ($\omega \approx 180°$) is favored by greater than 2.5 kcal/mol and χ_1 has a single broad minimum centered around 90° (Figure 2).

Pedersen, Suschitzky, and Itai have proposed that the origin of the trans-amide bond preference in *N*-methylacetanilide and other *N*-methylarylamides is a result of electronic repulsion between the electron-dense center of the phenyl ring and the

Scheme 3. Dihedral Angles in *N*-Aryl Peptoids[a]

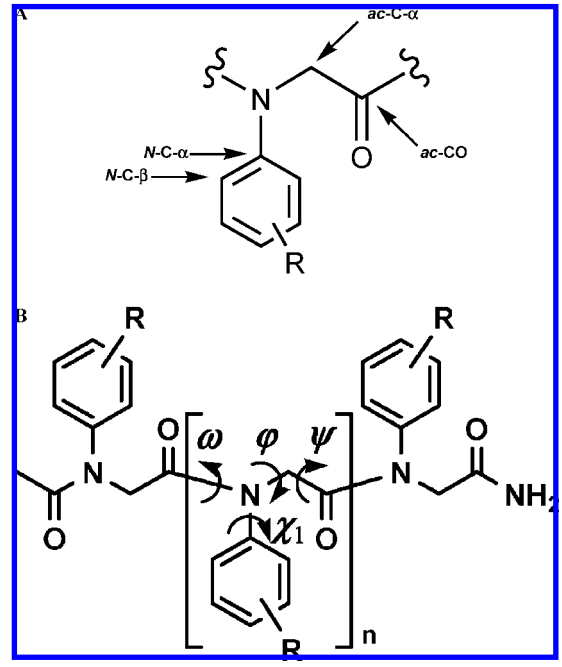

[a] (A) Atom labels within an *N*-aryl glycine monomer. (B) A representative *N*-aryl glycine peptoid oligomer with an acetylated *N*-terminus and amidated *C*-terminus. ω refers to the ac-C-$\alpha_{(i-1)}$, ac-$CO_{(i-1)}$, $N_{(i)}$, ac-C-$\alpha_{(i)}$ dihedral angle. φ refers to the ac-$CO_{(i-1)}$, $N_{(i)}$, ac-C-$\alpha_{(i)}$, ac-$CO_{(i)}$ dihedral angle. ψ refers to the $N_{(i)}$, ac-C-$\alpha_{(i)}$, ac-$CO_{(i)}$, $N_{(i+1)}$ dihedral angle. χ_1 refers to the ac-$CO_{(i-1)}$, $N_{(i)}$, N−C- $\alpha_{(i)}$, N−C- $\beta_{(i)}$ dihedral angle. For ortho- or meta-substituted *N*-phenyl side chains, N−C-β refers to the carbon atom closest to the substituent. The subscript (*i*) refers to a particular residue number.

(13) Bradley, E. K.; Kerr, J. M.; Richter, L. S.; Figliozzi, G. M.; Goff, D. A.; Zuckermann, R. N.; Spellmeyer, D. C.; Blaney, J. M. *Mol. Diversity* **1997**, *3*, 1–15.

(14) (a) Pedersen, B. F.; Pedersen, B. *Tetrahedron Lett.* **1965**, *34*, 2995–3001. (b) Pedersen, B. F. *Acta Chem. Scand.* **1967**, *6*, 1415–1424.

(15) (a) Garner, G. V.; Meth-Cohn, O.; Suschitzky, H. *J. Chem. Soc., C* **1971**, 1235–1236. (b) Itai, A.; Toriumi, Y.; Saito, S.; Kagechika Shudo, H. *J. Am. Chem. Soc.* **1992**, *114*, 10649–10650. (c) Saito, S.; Toriumi, Y.; Tomioka, N.; Itai, A. *J. Org. Chem.* **1994**, *60*, 4715–4720. (d) Yamasaki, R.; Tanatani, A.; Azumaya, I.; Saito, S.; Yamaguchi, K.; Kagechika, H. *Org. Lett.* **2003**, *5*, 1265–1267.

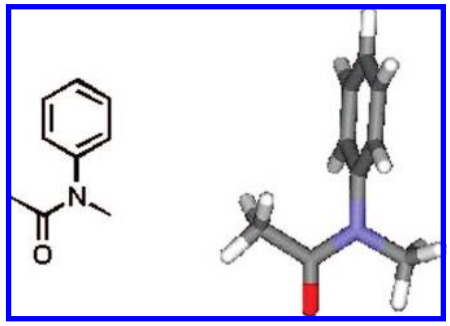

Figure 1. Model structure of *N*-methylacetanilide, optimized at the HF/6-31G* level of theory.

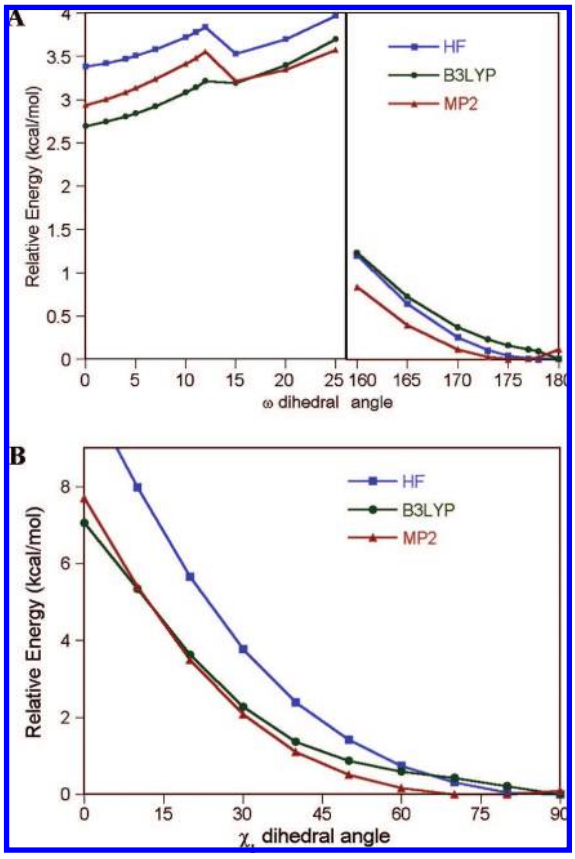

Figure 2. Quantum mechanics calculations of *N*-methylacetanilide: (A) Relative energy as a function of ω. Note that the region between 25° and 160° was not sampled because the amide nitrogen begins to assume a tetrahedral geometry in this region. (B) Relative energy as a function of χ_1. Note that ω was held fixed at 180°. For all plots, HF is HF/6-31G*//HF/6-31G*, B3LYP is B3LYP/6-311+G(2d,p)//HF/6-31G*, and MP2 is MP2/6-311+G(d,p)//HF/6-31G*.

amide oxygen, which would be in close proximity in the cis-isomer.[14,15] These studies suggest that various substituted *N*-methylacetanilides should retain trans-amide bond preference to varying degrees, depending on the electronic characteristics of the substituents. To test this hypothesis, the energy differences between cis and trans isomers of a set of substituted *N*-methylacetanilides (**1**–**10**) were calculated (Table 1). Each compound showed a substantial energetic preference for the trans-amide bond, ranging from 1.05 to 3.55 kcal/mol at the HF/G-31G* level of theory. Electron-withdrawing groups tended to decrease (and electron-donating groups increased) this preference.

Table 1. Energy Difference between Cis- and Trans-Amide Bonds in Substituted *N*-Methylacetanilides[a]

		$\Delta E_{cis\text{-}trans}$ (kcal/mol)		
Compd	Structure	HF	B3LYP	MP2
1	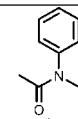	3.43	3.17	2.99
2	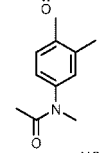	3.52	2.83	3.02
3	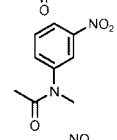	1.40	0.76	0.56
4	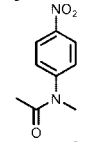	1.35	1.02	0.39
5	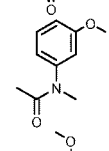	2.85	2.53	2.47
6	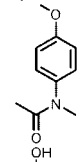	3.55	3.23	3.17
7	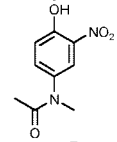	1.98	1.72	1.99
8	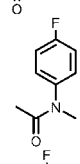	3.05	2.84	2.69
9	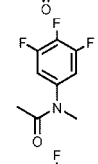	2.02	1.76	1.46
10	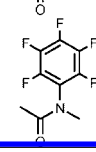	1.05	1.29	1.19

[a] Calculated using various *ab initio* quantum mechanics methods. HF is HF/6-31G*//HF/6-31G*, B3LYP is B3LYP/6-311+G(2d,p)//HF/6-31G*, and MP2 is MP2/6-311+G(d,p)//HF/6-31G*.

To verify this trend experimentally, a subset of the molecules found in Table 1 were synthesized, and their cis/trans-amide conformer ratios were analyzed in solution by nuclear magnetic resonance (NMR) spectroscopy (see Supporting Information). These compounds uniformly displayed a strong preference for populating the trans-amide bond geometry. For example, in deuterated methanol at 25 °C, *N*-methylacetanilide **1** existed as 92.9% trans-amide conformer. Compound **6**, bearing an electron-donating methoxy substituent, existed as 95.7% trans-amide conformer. Compound **8**, bearing an electron-withdrawing fluoro

Scheme 4. Structures of *N*-Aryl Peptoid Oligomers

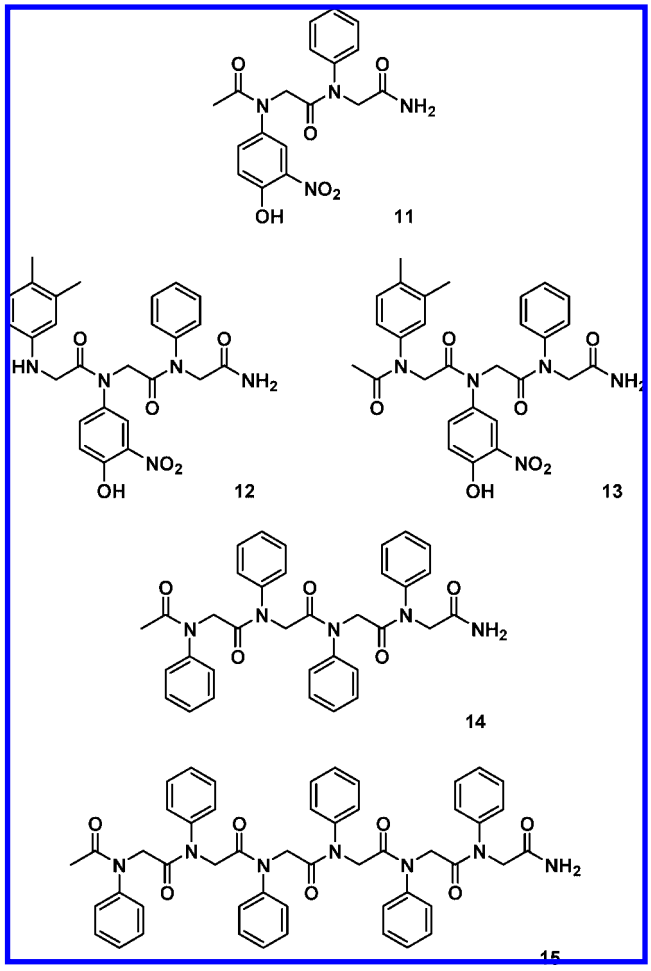

substitutent, existed as 91.9% trans-amide conformer. These data support the calculated structural trend reported in Table 1 and correspond with previously observed values in deuterated dichloromethane at −60 °C.[15d] The computational and experimental results collectively indicate that chemically diverse aromatic substituents can be incorporated into *N*-methylacetanilides while retaining the trans-amide bond conformer preference.

Synthesis of *N*-Aryl Peptoid Oligomers. Peptoid dimer **11** and trimers **12** and **13** (Scheme 4), bearing three unique *N*-phenyl side chains, were synthesized on Rink amide resin using a variation of the solid-phase submonomer protocol described by Zuckermann et al. (Scheme 5). [9] Typically, *N*-alkyl-substituted glycine units are generated by the iteration of successive short bromoacetylation and amine displacement steps (∼20 min). Given the deactivated character of aryl amines, however, longer reaction times are required.[9] After the first 20 min bromoacetylation, each subsequent amine displacement with an aryl amine was carried out for 16 h. All bromoacetylation reactions following substitution by an aryl amine were carried out for 90 min. When desired, the N-termini of peptoid oligomers were acetylated by a 90 min bromoacetylation reaction, followed by a 2 h hydride displacement with sodium borohydride in dimethylsulfoxide. Products were cleaved from the resin with aqueous trifluoroacetic acid. To confirm the applicability of this protocol to longer oligomer lengths, an acetylated *N*-(phenyl)-glycine homotetramer **14** and homohexamer **15** were also readily synthesized (Scheme 4). All peptoids were synthesized in good yield as determined by analytical reversed-phase high-performance liquid chromatography (see Figure 3 for representative RP-HPLC chromatogram, characteristic of *N*-aryl peptoid syntheses). Products were purified by RP-HPLC and their identities were confirmed by electrospray mass spectrometry.

Structural Characterization of *N*-Aryl Peptoid Oligomers. Peptoid dimer **11** was readily crystallized by slow evaporation in methanol. X-ray crystallographic studies of the plate-like crystals were conducted to determine a high-resolution crystal structure (Figure 4). The X-ray structure of peptoid dimer **11** confirms that the *N*-aryl-substituted backbone amide bonds are in the trans-amide bond geometry. Additionally, the values for the χ_1 side chain dihedral angles are also consistent with the computationally predicted rotamer (Table 2). The unit cell of the crystal contains four molecules including two pairs of identical structures in which the conformations from one pair are enantiomers of the corresponding pair. The molecules within the lattice pack to form a hydrogen-bonding network. In particular, each dimer and its adjacent enantiomer form a pair of intermolecular hydrogen bonds between the C-terminal amides and N-terminal carbonyl oxygens. In addition, each dimer and another enantiomer form a pair of hydrogen bonds between the C-terminal carbonyl oxygens and side chain phenol protons (see Supporting Information).

NMR spectroscopy was used to analyze the solution-phase structures of peptoids **11** and **13**. The conformational heterogeneity of each peptoid was assessed by 1-D ^{1}H NMR in deuterated acetonitrile and methanol. These experiments indicate that both oligomers exist as one substantially dominant conformation in solution (see Supporting Information). 2-D nuclear Overhauser effect spectroscopy (NOESY) was used to determine the geometry of the amide bonds in the major solution-phase conformer of each peptoid. Cis- and trans-amide bond geometries of oligo(*N*-aryl glycines) can be distinguished on the basis of distinct patterns of nuclear Overhauser effect interactions (NOEs) (see Supporting Information, Scheme S3). Specifically, the distance between backbone methylene protons of adjacent residues is typically between 3.0 and 3.5 Å in the cis geometry and between 4.5 and 5.0 Å in the trans geometry, the approximate threshold distance for NOE observations. Thus, the presence of a cis-amide bond should result in a substantial NOE between methylene protons of adjacent residues, whereas a trans-amide bond would preclude this cross-peak. Additionally, only the presence of a trans-amide bond would establish NOEs between the backbone methylene protons of one residue to the aromatic side chain ortho-protons of the C-terminal adjacent monomer. The NOESY spectra of peptoids **11** and **13** demonstrate a pattern of NOEs dictated by repeating trans-amide bonds throughout the backbone (see Supporting Information). These dominant conformers had greater than 90% abundance in solution relative to all observable conformers. Thus, NMR spectroscopy demonstrates that *N*-aryl peptoid oligomers exhibit conformational ordering distinguished by the presence of repeating trans-amide bonds.

Computational Studies of *N*-Aryl Peptoid Oligomers. Additional insights into the conformational behavior of *N*-aryl peptoids were obtained by a computational analysis of the energy landscape for the oligomer backbone conformations. Given the evidence for restricted side chain rotation ($\chi_1 \approx 90°$) and the strong tendency to form trans-amide bonds ($\omega \approx 180°$), we focused on evaluating the conformations available for the other rotatable backbone bonds defined by the φ and ψ dihedral angles. Thus, the structure of representative molecule **16** was studied, considering only φ and ψ as unknown rotational degrees

Scheme 5. Synthesis of *N*-Aryl Peptoid Oligomer **12**

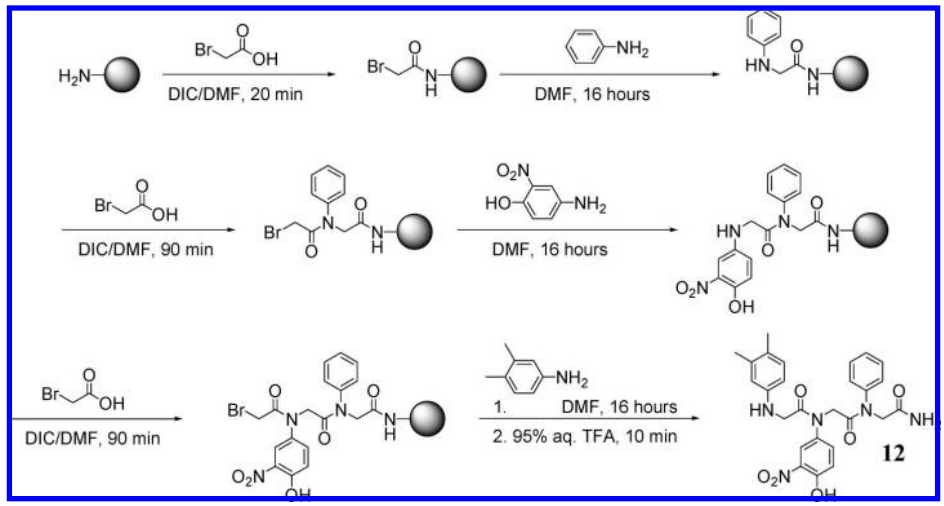

of freedom (Scheme 6). Compound **16** represents the smallest component of an *N*-aryl peptoid oligomer that includes interactions between neighboring side chains. We calculated a Ramachandran-type analysis of the conformational energy landscape for **16** by sampling both φ and ψ dihedrals at 15° increments through the entire range of possible values at the B3LYP/6-311+G(2d,p)//HF/6-31G* level of theory (Figure 5).[16] The resulting data show a center-symmetric landscape with two global minima around (φ,ψ) = A(60°,−150°) and B(−60°,150°). These two mirror image conformations, A and B, are at least 2 kcal/mol more stable than any other local minimum on the landscape.

In an *N*-aryl peptoid oligomer, either of these two local conformations could exist at each monomer position, leading to a potential mixture of secondary structures. However, molecular modeling studies of *N*-(phenyl)glycine hexamer **15** show that steric clashes make many combinations less likely to be populated. On the other hand, the repeating conformations $(A)_6$ and $(B)_6$ are energetically favorable and form extended right and left-handed helices, respectively (Figure 6). These secondary structures contain repeating *trans*-amide bonds and resemble the polyproline type II helix that is commonly observed in proline-rich protein sequences. The modeled helix has roughly 3.1 residues per turn and a helical pitch of approximately 9 Å per turn. The spacing between repeating aromatic side chains is sufficiently large to preclude significant aromatic/aromatic interactions. However, stabilizing n→π* interactions between adjacent trans-amide bonds may play a role in defining the overall conformation, as observed previously for polyproline type II structures.[11b,17]

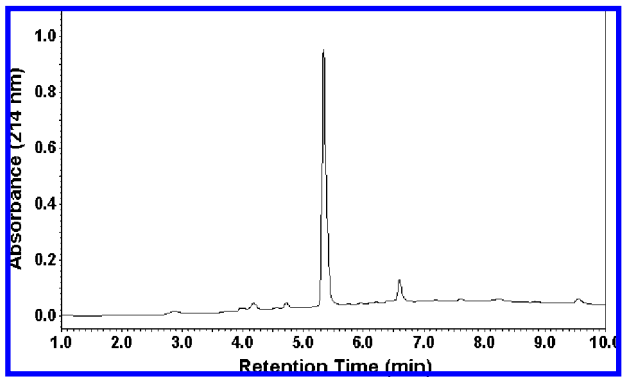

Figure 3. RP-HPLC chromatogram of crude peptoid **12**.

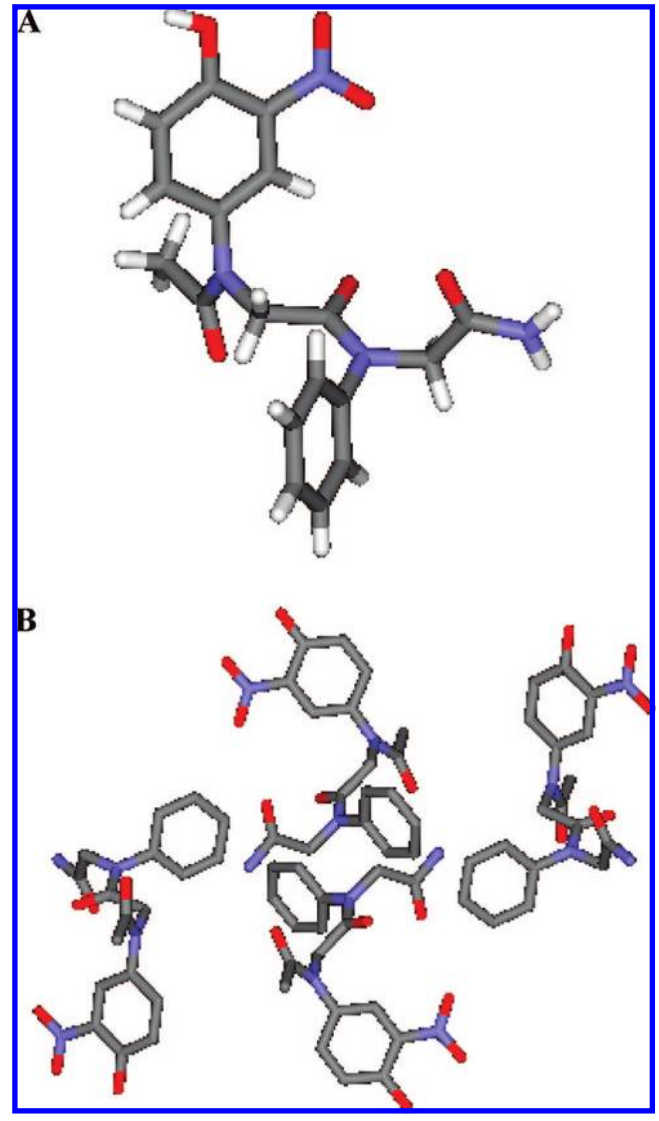

Figure 4. Crystal structure of peptoid dimer **11**: (A) single molecule; (B) unit cell (hydrogen atoms removed for clarity).

Table 2. Dihedral Angles Observed for Enantiomeric Chains in Dimer **11** Crystal Structure

chain	monomer	ω	φ	ψ	χ_1
A	*N*-(4-hydroxy-3-nitrophenyl)-glycine	177.45	80.27	−173.33	−100.59
	N-(phenyl)glycine	−175.68	95.98	162.81	111.82
B	*N*-(4-hydroxy-3-nitrophenyl)-glycine	−177.45	−80.22	173.34	100.59
	N-(phenyl)glycine	175.64	−95.98	−162.81	−111.82

Scheme 6. Structure of Compound **16**[a]

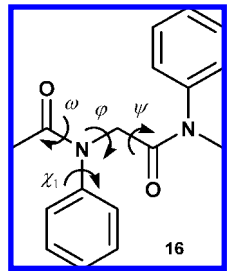

[a] Note that ω and χ_1 populate values near 180° and 90°, respectively (see Figure 2 and Scheme 3).

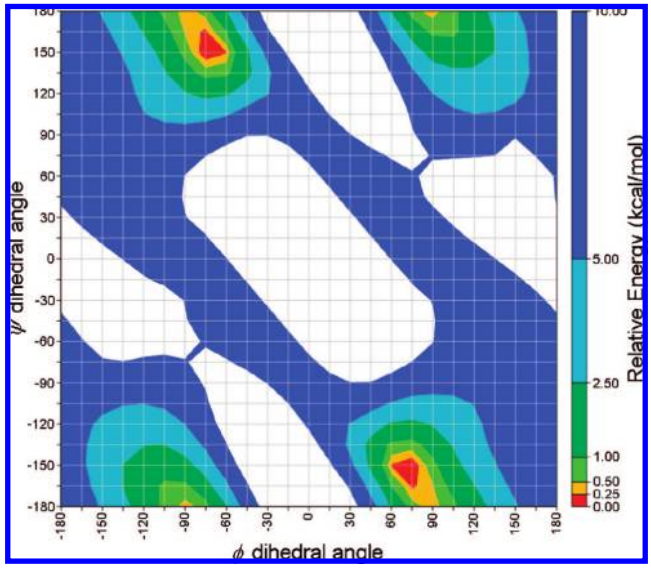

Figure 5. Ramachandran energy landscape of compound **16**. Relative energies (kcal/mol) are reported at the B3LYP/6-311+G(2d,p)//HF/6-31G* level of theory for structures every 15° in ϕ and φ. Regions in white are >10 kcal/mol above the lowest energy structure.

Cyclic Peptoids Bearing *N*-Aryl Glycine Units. Head-to-tail macrocyclization has proven to be an effective approach to generate novel, stable peptoid structures.[12a] In particular, cyclic *N*-alkyl peptoid hexamers and octamers form tight hairpin turns containing a mixture of cis- and trans-amide bonds. We explored the incorporation of *N*-aryl glycines into peptoid macrocycles and its effect on macrocycle structure. We anticipated that cyclic oligomers incorporating both *N*-alkyl and *N*-aryl glycine monomers would populate a combination of both cis- and trans-amide bonds throughout the backbone, and the placement of *N*-aryl glycines would site-specifically direct the formation of trans-amide bonds. Thus, cyclic peptoid hexamers **17** and **18** were synthesized from their linear precursors as previously described (see Supporting Information).[12a] The compounds were designed with two *N*-aryl side chains at positions (i and $i + 3$) or (i and $i + 1$), respectively (Scheme 7). A previously reported structure

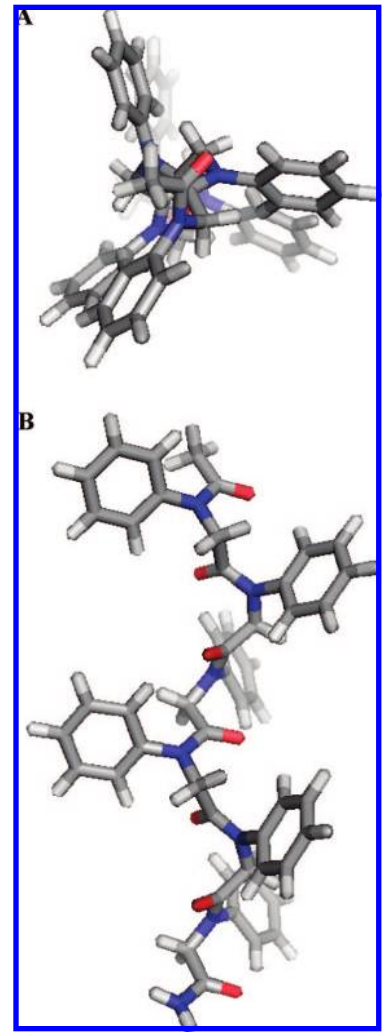

Figure 6. Model of *N*-(phenyl)glycine peptoid hexamer **15** (A, parallel to helix axis; B, perpendicular to helix axis) in a low energy conformation resembling a polyproline type II helix (see methods for details).

of a cyclic peptoid hexamer, incorporating exclusively *N*-alkyl side chains, displays a backbone amide bond motif that follows the pattern $(-\text{cis}-\text{cis}-\text{trans}-\text{cis}-\text{cis}-\text{trans}-)_{\text{cyclic}}$. Oligomer **17** was designed to mimic this motif, since the *N*-aryl side chains are three residues apart and should populate trans-amide bonds at these positions. By this rationale, oligomer **18** was designed to generate a different backbone motif with adjacent trans-amide bonds.

Peptoid macrocycle **17** was readily crystallized by slow evaporation from ethanol, and its high-resolution structure was determined by X-ray crystallography. The crystal structure of molecule **17** shows two trans-amide bonds at the sites with *N*-aryl substituents, and four cis-amide bonds at the other four locations. This pattern verified the initial prediction that *N*-aryl side chains preferentially direct trans-amide bond formation relative to *N*-alkyl side chains (Figure 7). The φ and ψ dihedral angles in both (*N*-phenyl)glycine monomers fall near the minima predicted in the landscape above (Table 3). In addition, the χ_1 dihedral angles for the *N*-aryl residues were 111.3° and 71.41°, within the range of the broad minimum predicted by computation of *N*-methylacetanilide (Figure 2B).

(16) Ramachandran, G. N.; Ramakrishnan, C.; Sasisekharan, V. *J. Mol. Biol.* **1963**, *7*, 95–99.
(17) Horng, J.-C.; Raines, R. T. *Protein Sci.* **2006**, *15*, 74–83.

Scheme 7. Structures of Cyclic Peptoids Containing *N*-Aryl and *N*-Alkyl Glycine Monomers

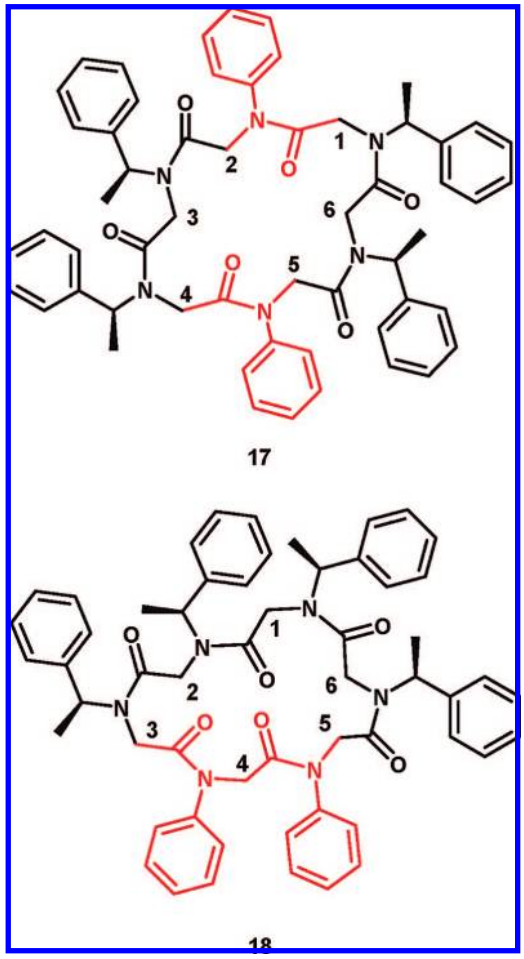

Cyclic peptoid **18** did not form crystals with dimensions necessary for X-ray diffraction. However, the macrocycle displayed conformational homogeneity in deuterated acetonitrile when analyzed by 1-D ^{1}H NMR (see Supporting Information). With additional HSQC, COSY, and ROESY NMR data, all of the backbone and non-aromatic side chain proton resonances for peptoid **18** were assigned. The HSQC data for compound **18** showed a series of interesting trends that provide insight into the structure of this molecule in solution (Figure 8). In particular, the ^{13}C shifts for the backbone methylene groups of the *N*-aryl glycine monomers (residues 4 and 5) are further downfield than those of the *N*-alkyl glycine monomers, making them readily distinguishable for spectral analysis. Additionally, the methine protons on the (*S*)-1-phenylethyl side chains are clustered into two distinct groups. ROESY data indicate that the three methine protons that are furthest downfield (methine protons at residues 1, 3, and 6) correspond to sites of cis-amide bonds, and the further upfield proton (methine proton at residue 2) corresponds to a trans-amide bond position (see Supporting Information). This observation is consistent with previously determined NMR structures of peptoids bearing (*S*)-1-phenylethyl side chains.[10c,18] The ROESY data establish that both *N*-phenyl-substituted amide bonds (**18**, residues 4 and 5) adopt a trans-conformation, as expected. The NMR study of cyclic peptoid **18** provided distance constraints that were used to generate a model backbone structure (see Supporting Information) containing three cis- and three trans-amide bonds (Scheme 7). This structure shows a novel cyclic scaffold in which the presence of adjacent trans-amide bonds was predicted a priori.

(18) Huang, K.; Wu, C. W.; Sanborn, T. J.; Patch, J. A.; Kirshenbaum, K.; Zuckermann, R. N.; Barron, A. E.; Radhakrishnan, I. *J. Am. Chem. Soc.* **2006**, *128*, 1733–1738.

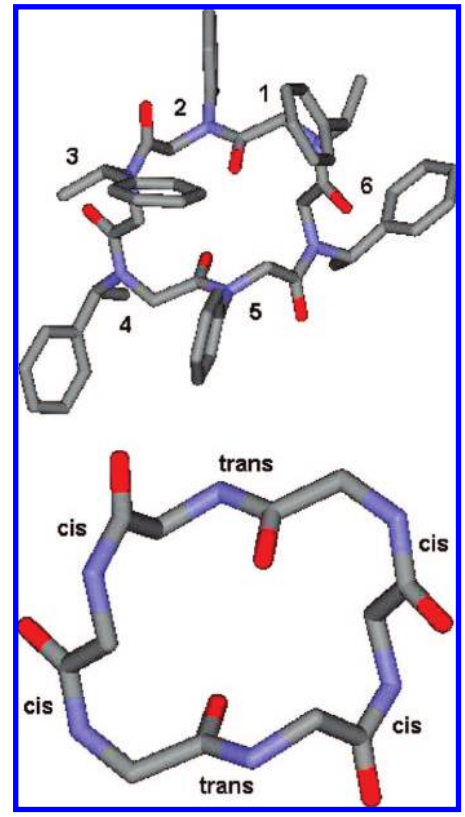

Figure 7. X-ray crystal structure of cyclic peptoid hexamer **17**. Bottom image includes only backbone atoms.

Table 3. Dihedral Angles Observed for Cyclic Hexamer **17** Crystal Structure

residue	monomer	ω	φ	ψ	χ_1
1	(S)-*N*-(1-phenylethyl)glycine	19.75	53.91	−162.24	−93.78
2	*N*-(phenyl)glycine	172.29	67.49	−139.44	111.3
3	(S)-*N*-(1-phenylethyl)glycine	16.31	−81.24	−179.8	−98.88
4	(S)-*N*-(1-phenylethyl)glycine	−5.51	−62.83	153.08	−125.37
5	*N*-(phenyl)glycine	−168.19	−72.49	139.03	71.41
6	(S)-*N*-(1-phenylethyl)glycine	−12.36	79.33	176.36	−138.13

Design Strategies for Peptoid Oligomers. As the capabilities to establish synthetic mimics of peptide secondary structures become more extensive, there is increasing interest in creating more sophisticated constructs akin to proteins. To be effective as protein mimics, however, a class of foldamers must exhibit the ability to support not only structural, but also chemical and functional diversity. Peptoids were among the first sequence-specific oligomers generated in combinatorial library format, as their solid-phase submonomer synthesis protocol facilitates the inclusion of chemically diverse *N*-alkyl and *N*-aryl side chains.[9,19] This synthetic ease has, in turn, led to the design of peptoids with interesting biological activities and materials properties.[20,21]

A modest-sized set of well-defined peptoid conformations has been described in the past several years.[20f] These biomimetic secondary structures include a polyproline type I helix generated by branched *N*-alkyl glycine oligomers,[5,10] a compact threaded loop stabilized by hydrogen bonding in a peptoid nonamer,[18]

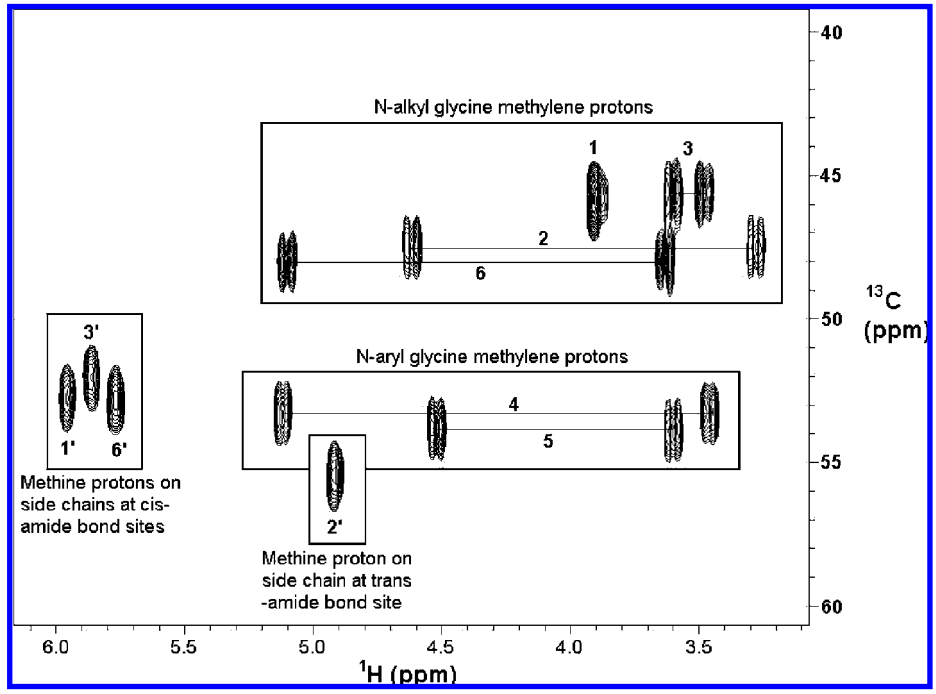

Figure 8. HSQC spectrum of cyclic hexamer **16** obtained from a 5 mM solution in acetonitrile-d_3 at room temperature.

and macrocyclic peptoid hairpins that mimic a protein β-turn motif.[12a] In this study, we demonstrate the ability to restrict peptoid backbone conformational space to the same regions found in protein polyproline type II helices. The ability to design peptoids with complex functions will ultimately rely on the combination of secondary structural elements into more elaborate tertiary and quaternary structures. The growing collection of secondary structures now described for peptoids should provide the building blocks to generate these higher-order architectures.

Conclusion

In this report, we describe the conformational preferences of *N*-aryl glycine peptoids. Oligomers from dimer to hexamer length were efficiently synthesized on solid-phase. The relative energies of cis- and trans-amide bonds in these molecules were evaluated by computational methods, and the energetic preference for trans-amide bond conformers was shown to tolerate a wide array of aryl substituents. The structures of *N*-aryl peptoid oligomers were studied by solution NMR spectroscopy and X-ray crystallography. These studies confirm that the compounds prefer trans-amide bonds along the backbone and exhibit the predicted side chain rotamers. Additional computational studies indicate that the critical rotatable bonds in *N*-aryl peptoid oligomers (ω, χ_1, φ, and ψ) have energetic preferences which lead to well-defined conformations, notably a structure resembling that of a polyproline type II helix.

The de novo design of functional foldamers will depend on the ability to predict structure from sequence. Here, we have shown that *N*-aryl glycine monomer units provide a means to achieve this goal in peptoids. The local conformations of *N*-aryl glycine oligomers are well-defined and promote backbone conformational stability. The ability to direct the presence of trans-amide bonds at any location within a peptoid sequence will enhance the capacity to predict overall backbone structure, as evidenced in the successful design of *N*-alkyl/*N*-aryl hybrid cyclic hexamers. Peptoids provide an attractive platform for access to chemically diverse molecular architectures. The use of *N*-aryl glycine monomer units in conjunction with other strategies may ultimately allow for the development of predictable structure–function relationships in this important class of peptidomimetic foldamers.

Experimental Section

Materials. Bromoacetic acid, aniline, 4-amino-2-nitrophenol, 4-methoxyaniline, 4-nitroaniline, 4-fluoroaniline, piperidine, citric acid, iodomethane, and sodium hydride (60% w/w dispersion in mineral oil) were purchased from Sigma-Aldrich (St. Louis, MO). *S*-(−)-1-phenylethylamine was purchased from TCI (Portland, OR). *N*,*N*′-Diisopropylcarbodiimide, *N*,*N*-diisopropylethylamine (DIEA), and 1,1,1,3,3,3-hexafluoro-2-propanol (HFIP) were purchased from Chem-Impex International (Wood Dale, IL). Trifluoroacetic acid was purchased from Acros (Belgium). PyBOP, Fmoc-protected Rink amide resin (0.69 mmol·g^{-1} loading level) and 2-chlorotrityl resin (1.3 mmol·g^{-1} loading level) were purchased from Nova Biochem (San Diego, CA).

Synthesis of N-Methylacetanilides (1, 2, 4, 6, and 8). Aniline or an aniline derivative (1 mmol) was dissolved in 2 mL of dry

(19) (a) Horn, T.; Lee, B.-C. ; Dill, K. A.; Zuckermann, R. N. *Bioconjugate Chem.* **2004**, *15*, 428–435. (b) Lee, B.-C.; Zuckermann, R. N.; Dill, K. A. *J. Am. Chem. Soc.* **2005**, *127*, 10999–11009.

(20) (a) Patch, J. A.; Kirshenbaum, K.; Seurynck, S. L.; Zuckermann, R. N.; Barron, A. E. *Pseudo-peptides in Drug Discovery*; Nielsen, P.E. Ed.; Wiley-VCH: Weinheim, Germany, 2004; pp 1−35. (b) Utku, Y.; Dehan, E.; Ouerfelli, O.; Piano, F.; Zuckermann, R. N.; Pagano, M.; Kirshenbaum, K. *Mol. BioSyst.* **2006**, *2*, 312–317. (c) Holub, J. M.; Garabedian, M. J.; Kirshenbaum, K. *QSAR Comb. Sci.* **2007**, *26*, 1175–1180. (d) Lim, H.-S.; Archer, C. T.; Kodadek, T. *J. Am. Chem. Soc.* **2007**, *129*, 7750–7751. (e) Chongsiriwatana, N. P.; Patch, J. A.; Czyzewski, A. M.; Dohm, M. T.; Ivankin, A.; Gidalevitz, D.; Zuckermann, R. N.; Barron, A. E. *Proc. Natl. Acad. Sci. U.S.A.* **2008**, *105*, 2794–2799. (f) Yoo, B.; Kirshenbaum, K *Curr. Opin. Chem. Biol.* **2008**, xx. doi:10.1016/j.cbpa.2008.08.015.

(21) (a) Statz, A. R.; Meagher, R. J.; Barron, A. E.; Messersmith, P. B. *J. Am. Chem. Soc.* **2005**, *127*, 7972–7973. (b) Shah, N. H.; Kirshenbaum, K. *Macromol. Rapid Commun.* **2008**, *29*, 1134–1139.

dichloromethane. Acetic anhydride (189.05 μL, 2 mmol) and DIEA (522.53 μL, 3 mmol) were added to the solution and the mixture was stirred at room temperature until the aniline was no longer evident by thin layer chromatography in 10% ethyl acetate in dichloromethane (reaction times varied from 2 to 18 h depending on the aromatic substituent). Next, 2 mL of dichloromethane were added to the reaction mixture, and the solution was washed twice with 5 mL of 10% w/w aqueous citric acid.

After washing, the organic layer was dried under reduced pressure, and the residue was redissolved in 4 mL of dry *N,N*-dimethylformamide (DMF). Sodium hydride dispersed in mineral oil (100 mg, 2.5 mmol) and iodomethane (155.64 μL, 2.5 mmol) were added to the solution, and the mixture was stirred overnight. The DMF was then removed under reduced pressure, and the remaining residue was dissolved in 4 mL of dichloromethane. This solution was then washed twice with 5 mL of 10% w/w citric acid, and the organic layer was dried under reduced pressure. The residue was then redissolved in 4 mL of methanol and extracted twice with 5 mL of hexane. The methanol was removed under reduced pressure, and the remaining residue was lyophilized to a powder. Products less than 95% purity (based on NMR) were purified on a silica gel column with a gradient of 5−50% ethyl acetate in dichloromethane. Products were analyzed and confirmed by electrospray mass spectrometry and NMR (see Supporting Information). The desired compounds were isolated in the following yields: **1**, 20.1%; **2**, 8.5%; **4**, 41.7%; **6**, 24.6%; and **8**, 37.7%.

***N*-Aryl Peptoid Synthesis.** Solid-phase synthesis of peptoid oligomers was carried out in fritted syringes on Rink amide resin using a variation of the peptoid submonomer synthesis reported by Zuckermann et al.[9] N-Substituted glycine monomers were generated from their corresponding amine submonomers. *N*-(phenyl)glycine was generated by incorporation of aniline. *N*-(3,4-Dimethylphenyl)glycine was generated by incorporation of 3,4-dimethylaniline. *N*-(4-Hydroxy-3-nitrophenyl)glycine was generated by incorporation of 4-amino-2-nitrophenol. (*S*)-*N*-(1-Phenylethyl)glycine was generated by incorporation of S-(−)-1-phenylethylamine. All equivalencies are given with respect to resin loading level.

In a typical oligomer synthesis, 100 mg of resin with a loading level of 0.69 mmol·g^{-1} was swollen in 2 mL of *N,N′*-dimethylformamide (DMF) for 30 min. Following swelling, the Fmoc protecting group was removed by treatment with 1.5 mL of 20% piperidine in DMF twice for 20 min. After deprotection and after each subsequent synthetic step, the resin was washed twice with 2 mL of DMF, twice with 2 mL of dichloromethane, and twice again with 2 mL of DMF, one minute per wash.

Peptoid synthesis was carried out with alternating bromoacylation and amine displacement steps. For each bromoacylation step, 20 equiv bromoacetic acid (1.2 M in DMF) and 24 equiv *N,N′*-diisopropylcarbodiimide (neat) were added to the resin, and the mixture was agitated for 90 min, except for the first bromoacetylation, which was carried out for only 20 min. After washing, 20 eq. of the required amine (1.0 M in DMF) were added to the resin and agitated for 16 h. When required, peptoid *N*-termini were acetylated on solid-phase by the following method. First, the N-terminus was bromoacetylated for 90 min as described above. After washing, the bromide was displaced by adding 5 eq. of sodium borohydride (0.25 M in dimethylsulfoxide) to the resin and agitating the mixture for 2 h.

Peptoid Macrocycle Synthesis. Linear peptoid precursors for macrocyclization were synthesized on 2-chlorotrityl resin similar to the procedure described above (See Supporting Information for linear structures). For the first bromoacetylation step, 100 mg of resin were suspended in 5 equiv bromoacetic acid (1.0 M in dry dichloromethane) and 20 equiv DIEA (neat) and agitated for 30 min. For each successive bromoacetylation, 20 equiv bromoacetic acid (1.2 M in DMF) and 24 equiv *N,N′*-diisopropylcarbodiimide (neat) were added to the resin, and the mixture was agitated for 20 min following displacements with S-(−)-1-phenylethylamine or 90 min following displacements with aniline. Amine submonomers were allowed to react with the resin after each bromoacetylation step. The resin was mixed with 20 equiv S-(−)-1-phenylethylamine (1.0 M in DMF) and agitated for 20 min or mixed with 20 equiv aniline (1.0 M in DMF) and agitated for 16 h. When the desired sequence was achieved, linear peptoid products were cleaved from the resin by treatment with 20% HFIP in dichloromethane (40 mL·g^{-1} resin) for 30 min. After filtration, the cleavage cocktail was concentrated by rotary evaporation under reduced pressure for large volumes or under a stream of nitrogen gas for volumes less than 1 mL. Cleaved samples were then resuspended in 50% acetonitrile in water and lyophilized to powders.

A typical cyclization was conducted with the purified linear products in dry, deoxygenated DMF. The linear oligomer (24 μmol) was suspended in 10.50 mL of DMF in a 50 mL conical tube. PyBOP solution (750 μL of 96 mM PyBOP freshly prepared in DMF) and DIEA solution (750 μL of 192 mM DIEA freshly prepared in DMF) were added to the peptoid. The reaction vessel was flushed with nitrogen and sealed to exclude air. The reaction proceeded overnight at room temperature, and 10 μL of reaction mixture were diluted with 140 μL of 50% ACN in H_2O to quench the reaction. The diluted sample was analyzed by HPLC to confirm completion. After the allotted reaction time, DMF was removed by lyophilization, and the samples were resuspended in 50% aqueous acetonitrile for purification.

Peptoid Characterization and Purification. Peptoid products were cleaved from the Rink amide resin by treatment with 95% aqueous trifluoroacetic acid for 10 min (40 mL·g^{-1} resin). After filtration, the cleavage cocktail was concentrated by rotary evaporation under reduced pressure for large volumes or under a stream of nitrogen gas for volumes less than 1 mL. Cleaved samples were then resuspended in 50% acetonitrile in water to the desired concentration.

Peptoid oligomers were characterized by analytical reversed-phase high performance liquid chromatography (RP-HPLC) using an analytical C_{18} column on a Beckman Coulter System Gold HPLC system. Products were detected by UV absorbance at 214 nm during a linear gradient from 5 to 95% solvent B (0.1% trifluoroacetic acid in HPLC-grade acetonitrile) in solvent A (0.1% trifluoroacetic acid in HPLC-grade water) in 10 min with a flow rate of 0.7 mL·min^{-1}. The expected molecular mass of each product was confirmed using liquid chromatography−mass spectrometry (LC−MS) on an Agilent 1100 series LC/MSD trap XCT with an electrospray ion source in positive ion mode.

Peptoid products were purified to >95% purity using the same RP-HPLC apparatus described above with a preparatory C_{18} column. Products were detected by UV absorbance at 230 nm during a linear gradient from 5 to 95% solvent B in solvent A in 50 min with a flow rate of 2.5 mL·min^{-1}. Compounds were then lyophilized to powders.

NMR Spectroscopy. 1-D proton spectra were obtained using either a Bruker 400 MHz NMR spectrometer, a Bruker 500 MHz NMR spectrometer, or a Varian 500 MHz NMR spectrometer. Multidimensional data were obtained using either a Bruker 500 MHz NMR spectrometer or a Varian 500 MHz NMR spectrometer. NMR experiments were carried out at either 25 or 0 °C. All NMR samples were prepared as 5−10 mM solutions in CD_3CN or CD_3OD. NMR spectra of the CD_3OD solutions were measured on the Varian 500 MHz spectrometer in Shigemi tubes. To increase resolution in the indirectly detected dimension, some NOESY spectra were measured with BASHD-NOESY pulse sequences.[22]

Crystallization of 11. Compound **11** (5 mg in 500 μL of HPLC grade methanol) was filtered through a 0.5 μm stainless steel syringe tip filter. The solution was then allowed to evaporate slowly at room temperature to form crystals. Crystallography data: yellow plate-

(22) (a) Krishnamurthy, V. V. *Magn. Reson. Chem.* **1997**, *35*, 9–12. (b) Kaerner, A.; Rabenstein, D. L. *Magn. Reson. Chem.* **1998**, *36*, 601–607.

like crystal, 0.32 × 0.20 × 0.03 mm^3, monoclinic, $P2(1)/c$, a = 10.3748(15) Å, b = 15.862(3) Å, c = 10.7396(16) Å, $\alpha = 90°$, β = 99.820(4)°, $\gamma = 90°$, $Z = 4$, V = 1741.5(5) Å^3, ρ_{calcd} = 1.474 g/cm^3. X-ray diffraction data were collected on a Bruker Apex II X-ray diffractometer.

Crystallization of 17. Compound **17** (5 mg in 500 μL of HPLC grade ethanol) was filtered through a 0.5 μm stainless steel syringe tip filter. The solution was then allowed to evaporate slowly at room temperature to form crystals. Crystallography data: colorless needle-like crystal, 0.28 × 0.21 × 0.12 mm^3, monoclinic, $P2(1)$, a = 9.7832(3) Å, b = 14.8225(4) Å, c = 16.4479(5) Å, $\alpha = 90°$, β = 91.127(2)°, $\gamma = 90°$, $Z = 2$, V = 2384.67(12) Å^3, ρ_{calcd} = 1.269 g/cm^3.

Computational Studies. All QM calculations were done with the Gaussian 2003 package.[23] All calculations used the "SCF=Tight" option and all MP2 calculations used the "full" option. Basis sets and constrained degrees of freedom are noted in the text and legends. The model of the *N*-(phenyl)glycine hexamer was generated using the SIgMA package.[24] A force field was generated by adapting parameters from the cedar all-atom energy function.[25] Backbone torsions where held at predicted minima (φ at −60° and ψ at 150°) by 20 kcal/mol harmonic restraints, and structure was subject to several thousand cycles of energy minimization. The structures were then further optimized using the semiempirical self-consistent-charge density functional tight-binding (SCCDFTB) model with 6 × 20 rounds of restrained minimization followed by 6 × 20 rounds of minimization without external restraints.[26]

Acknowledgment. We thank Dr. Chin Lin for his helpful discussions on peptoid NMR characterization. We also acknowledge Dr. Sam Hawxwell for his helpful conversations regarding crystallization techniques and for aiding in X-ray diffraction studies of compound **17**. We thank Airon Soegiarto for contributing to the X-ray crystallography of compound **11** and Doug Renfrew for assisting with QM work. This work was supported by a National Science Foundation CAREER Award (CHE-0645361). We also thank the NCRR/NIH for a Research Facilities Improvement Grant (Grant C06RR-165720) at NYU.

Supporting Information Available: Complete ref 23; designator abbreviations for *N*-substituted glycine peptoid monomers; NMR and mass spectrometry characterization of synthesized *N*-methylacetanilides; mass spectrometry and RP-HPLC characterization data for compounds **11**−**15**, **17**, and **18**; additional representations of the crystal structures of dimer **11** and cyclic hexamer **17**; 1-D and 2-D NMR spectra of compounds **11**, **13**, **17**, and **18**; NMR-based model structure of cyclic hexamer **18**; additional computational data; and additional visualizations of the Ramachandran-like conformational analysis of **16**. This material is available free of charge via the Internet at http://pubs.acs.org.

JA804580N

(23) Frisch, M. J.; et al. *Gaussian 03*; Gaussian, Inc.: Wallingford, CT, 2004.

(24) Mann, G.; Yun, R. H.; Nyland, L.; Prins, J.; Board, J.; Hermans, J. *Computational Methods for Macromolecules: Challenges and Applications*; Schlick T., Gan, H. H., Eds.; Springer-Verlag: Berlin, Germany, 2002; pp 129−145.

(25) (a) Hermans, J.; Berendsen, H. J. C.; van Gunsteren, W. F.; Postma, J. P. M. *Biopolymers* **1984**, *23*, 1513–1518. (b) Ferro, D. R.; McQueen, J. E.; McCown, J. T.; Hermans, J. *J. Mol. Biol.* **1980**, *136*, 1–18.

(26) (a) Elstner, M.; Frauenheim, T.; Kaxiras, E.; Seifert, G.; Suhai, S. *Phys. Status Solidi B* **2000**, *217*, 357–376. (b) Hu, H.; Elstner, M.; Hermans, J. *Proteins* **2003**, *50*, 451–463.